Nucleon and Nuclear Structure Studies in Electroproduction with the CLAS Detector at Jefferson Lab

Stepan Stepanyan (Jefferson Laboratory) for the CLAS Collaboration
(Dated: January 27, 2017)

A diverse program for studying the structure of nucleons and nuclei is underway using the CEBAF Large Acceptance Spectrometer (CLAS) at Jefferson Lab. A wealth of data has been obtained in inclusive, semi-inclusive, and exclusive electroproduction reactions using a variety of unpolarized and polarized beams and targets. The results include studies of excited nucleon states, measurements of nucleon, proton and neutron Form Factors (FFs), Parton Distribution Functions (PDFs), Transverse Momentum Distributions (TMDs), and Generalized Parton Distributions (GPDs), as well as Short Range Correlations (SRCs) in nuclei and Color Transparency phenomena.

Jefferson Lab's electron accelerator, CEBAF, doubled its energy to 12 GeV and the upgrade of the experimental equipment is near completion in the experimental halls. The upgraded CLAS detector, CLAS12, enables execution of a broader physics program, with the main focus on uncovering the TMDs and GPDs using semi-inclusive and exclusive reactions in a new kinematic domain. In this talk, an overview of the CLAS electroproduction measurements with 6 GeV CEBAF and prospects of nucleon and nuclear structure studies with the 12 GeV machine and the CLAS12 detector will be discussed.

PACS numbers: 13.60.-r; 13.60.Fz; 13.60.Hb; 13.60.Le; 25.30.-c

I. CLAS DETECTOR AT JEFFERSON LAB

The CLAS detector at Jefferson Lab is a multi-purpose, large acceptance spectrometer consisting of Drift Chambers, Scintillator Counters, gas threshold Cherenkov Counters, and Electromagnetic Calorimeters [1]. Tracking and identification of stable charged particles are performed in the laboratory polar angular range from 8° to 140°. The PID system allows π/K separation up to 2 GeV and π/p up to 3 GeV. For detection and identification of neutrons and photons, electromagnetic calorimeters in the forward region are used.

CLAS runs experiments with polarized electron and photon beams, using a variety of solid and liquid targets, as well as longitudinally polarized targets. In electron experiments, instantaneous luminosity of about 2×10^{34} cm^{-2}s^{-1} has been achieved. Over 15 years the CLAS Collaboration executed a broad physics program that included studies of nucleon structure using elastic and deep inelastic scattering, hadron spectroscopy, in medium effects, and nuclear structure. Most of the physics program will continue with the upgraded CEBAF using up to 11 GeV polarized electron beams and the new CLAS12 detector. In Fig. 1, the kinematic reach of CLAS12 at 11 GeV is shown together with 6 GeV CLAS and other facilities. With an 11 GeV beam, CLAS12 will extend studies of nucleon structure to higher $x_B = Q^2/(2p \cdot q)$ and $Q^2 = (k' - k)^2$ where k (k') is the incoming (scattered) electron four vector. In this report, highlights of a few selected topics of the CLAS physics program with electron beams and the new prospectives with the upgraded CEBAF and CLAS12 will be presented.

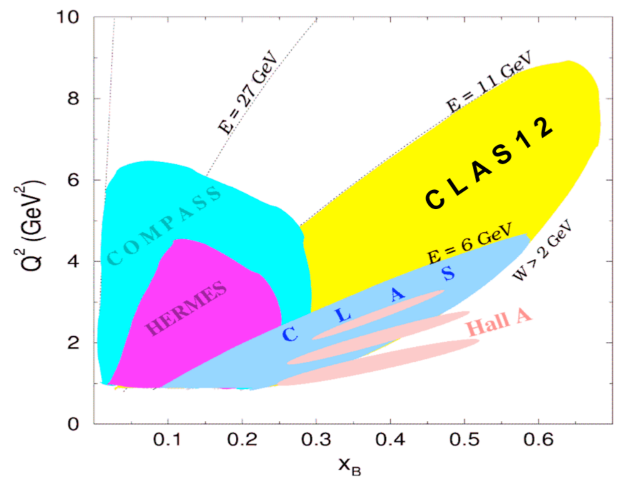

FIG. 1. Kinematic coverage in terms of Q^2 and x_B for CLAS and CLAS12 in comparison with various other detectors.

II. 3D-STRUCTURE OF THE NUCLEON

The formalisms of Transverse Momentum Distributions (TMDs) [2] and Generalized Parton Distributions (GPDs) [3] provide a framework for the three-dimensional imaging of the nucleon and nucleus experimentally using Deeply Virtual Semi-Inxclusive and Exclusive processes. In leading-twist, there are four quark GPDs (H, $\tilde{H}$, E, $\tilde{E}$) that describe exclusive processes. GPDs are hybrid distributions that combine aspects of the usual collinear PDFs and elastic form factors. As such, GPDs simultaneously encode information on parton distributions and correlations in both momentum (in the longitudinal direction) and coordinate (in the transverse direction) spaces, and they offer exciting opportunity for determination of the total angular momentum carried by quarks inside the nucleon via Ji's sum rule.

Deeply Virtual Compton Scattering (DVCS), electroproduction of real photons via $ep \to e'p'\gamma$ in the deep inelastic scattering regime, is the simplest and cleanest reaction to access GPDs experimentally. After the first pioneering measurements of the beam [4] and target [5] spin asymmetries in DVCS using available CLAS data, a wealth of data on single (BSA and TSA) and double spin (DSA) asymmetries, and cross sections have been obtained in dedicated DVCS experiments with CLAS [6–8]. The kinematic dependencies of the obtained asymmetries and cross sections were compared to the predictions of GPD models and put important constraints on the GPD parameterizations. These large sets of measured asymmetries and cross sections were used to extract Compton Form Factors (CFFs), which contain GPDs, using global fitting methods. In Fig. 2 one such extraction of the imaginary part of the $\mathcal{H}_{Im}$ and $\tilde{\mathcal{H}}_{Im}$ CFFs is presented from Ref. [7]. In the figure the transferred momentum squared (t) dependence of the extracted CFFs from the fit to TSA, BSA, and DSA data is shown for several bins of Q^2 and x_B. The CLAS data in a wide range of kinematics improves the precision of the extraction significantly. In Fig. 3 a similar extraction of the real and imaginary parts of the $\mathcal{H}$ CFF from fits to the unpolarized cross sections and beam-polarized cross section differences are shown from Ref. [8]. In the figure, VGG model calculations are shown as well.

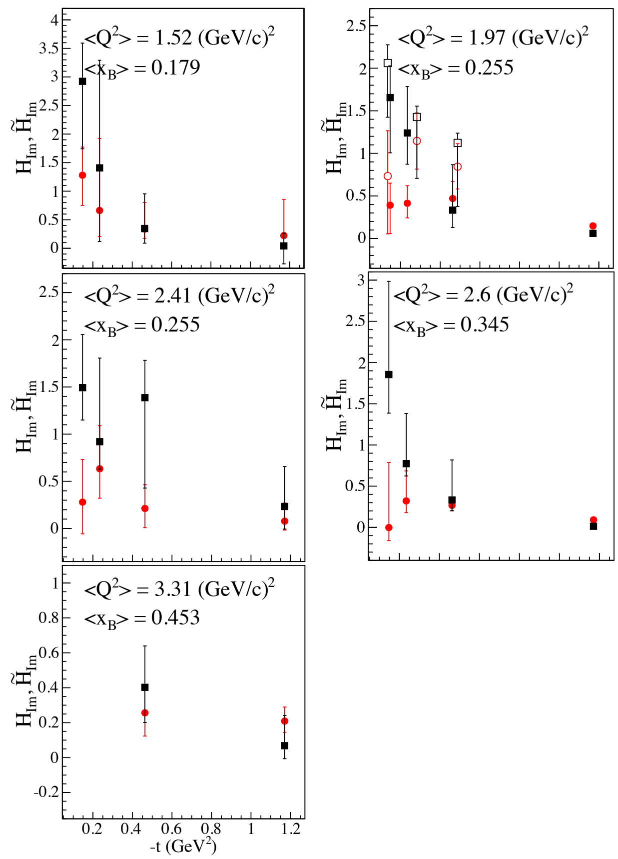

FIG. 2. t dependence for each Q^2-x_B bin of H_{Im} (black squares) and $\tilde{H}_{Im}$ (red circles). The full points are obtained by fitting the CLAS TSA, BSA, and DSA data. The empty points were obtained by fitting the BSA results from Ref. [6] integrated over all values of Q^2 at $x_B \sim 0.25$ and the TSAs from Ref. [5].

The beam spin asymmetry in DVCS has also been studied with nuclear targets. For the first time, using a low energy recoil detector, a Radial Time Projection Chamber (RTPC) based on GEM technology, beam spin asymmetries were measured on ^{4}He in the fully exclusive final state. Since ^{4}He is a spin-0 object, in leading twist only one GPD (H) is needed to define its partonic structure.

$$A_{LU} = \frac{\alpha \Im\mathrm{m}\mathcal{H}}{\alpha_1 + \alpha_2 \Re\mathrm{e}\mathcal{H} + \alpha_3(\Im\mathrm{m}(\mathcal{H})^2 + \Re\mathrm{e}(\mathcal{H})^2))} \quad (1)$$

The DVCS on a spin-0 target allows a model-independent extraction of the real and imaginary parts of CFF $\mathcal{H}$ from the beam spin asymmetry measurements. In Fig. 4 the ϕ dependence of the BSA $A_{LU}^{^4He}$ is shown for one bin of Q^2, x_B, and t. The red line is the fit to the data with the function in Eq.1 where $\Im\mathrm{m}\mathcal{H}$ and $Re\mathcal{H}$ are the free parameters. The kinematic dependencies of CFF have been obtained and compared with model predictions [9].

III. NUCLEON FORM FACTORS

The elastic electromagnetic form factors (FFs) are one of the fundamental observables that describe the internal structure of the nucleon. The evolution of FFs with Q^2 characterizes the distributions of charge and magnetization within the proton and neutron. While the proton elastic FFs are measured up to very high Q^2 with high precision in many experiments, data on neutron FFs are scarce. Taking advantage of the large coverage and relatively high efficiency of the CLAS calorimeters for neutron detection, G_M^n was measured with CLAS using a liquid-deuterium target in the range $Q^2 = 1.0-4.8$ GeV^2. In Fig. 5 the CLAS results on $G_M^n/\mu_n G_D$ are shown together with the available world's data [10]. The experiment measured the ratio of quasi-elastic scattering on the neutron and the proton, and G_M^n was extracted from the ratio using the known proton electric and magnetic FFs, and the calculated value (small) for G_E^n. As this was a ratio measurement, uncertainties due to nuclear effects largely cancel out. The CLAS measurements of G_n^M are the only high precision measurements for Q^2 above 1 GeV^2. The CLAS Collaboration has an approved experiment with CLAS12 to continue the G_M^n measurements for Q^2 up to 13 GeV^2 using an 11 GeV beam.

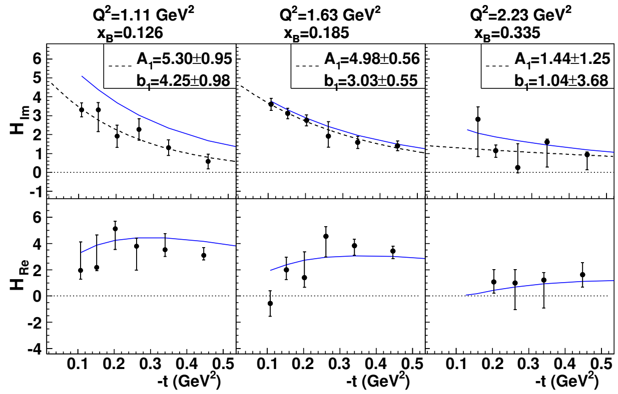

FIG. 3. Results of the CFF fit of DVCS cross section data for H_{Im} (upper panel) and H_{Re} (lower panel), with only the GPDs H and $\tilde{H}$, for three of our (Q^2, x_B) bins, as a function of t. The blue solid curves are the predictions of the VGG model. The black dashed curves show the fit of the results with the function Ae^{bt}.

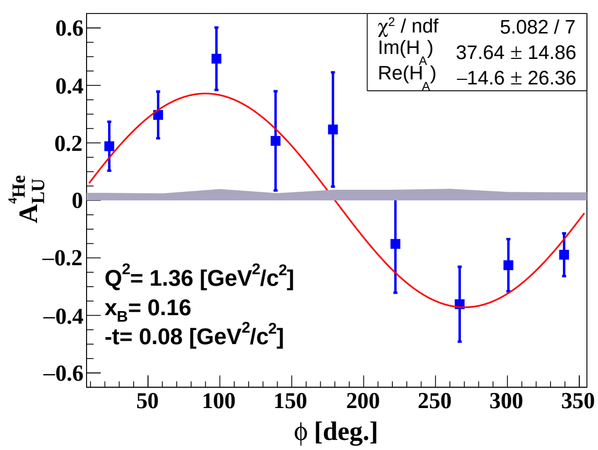

FIG. 4. The beam spin asymmetry in coherent DVCS on ^{4}He as a function of ϕ for one kinematic point in Q^2, x_B, and t. The error bars represent the statistical uncertainties. The shaded band represents the systematic uncertainties. The red curve represents the fit with the function in Eq.1.

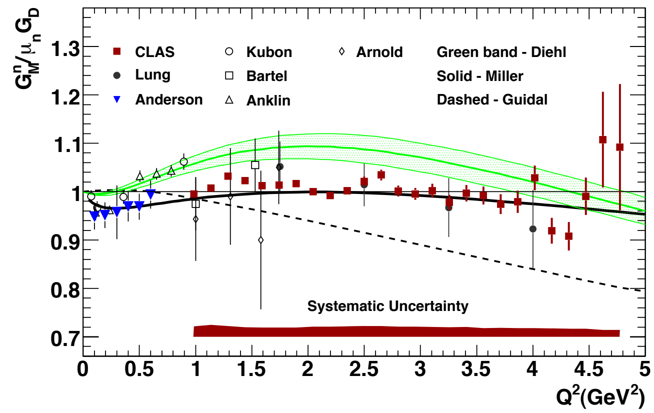

FIG. 5. The neutron magnetic form factor G_M^n in units of $\mu_n G_D$ as a function of Q^2.

IV. THE STRUCTURE OF THE FREE NEUTRON

A large amount of precision data on the partonic structure of the proton has been obtained in deep inelastic electron scattering. A similar measurement for the neutron, obtained using nuclear targets, has large uncertainties due to nuclear effects. Using the low energy spectator proton tagging method, high precision deep inelastic electron scattering measurements on almost free neutrons have been performed using CLAS. Spectator protons were detected in the backward direction using an RTPC. A high pressure gaseous deuterium target was separated from the RTPC detection volume by thin foils that allowed for tagging of protons down to 0.07 GeV momenta.

In Fig. 6 from Ref. [11] the ratio of F_2 structure functions of the neutron and the proton (F_2^n/F_2^p) is shown. In the DIS region, measurements reach up to $x^* = 0.56$, at Q^2=4 GeV^2, where x^* (as well W^* in the caption of the figure) is calculated with the target neutron four momentum deduced from momentum-energy conservation using the spectator proton three momentum. This ratio is related to the d/u ratio in the proton that has definite values in different models. The simplest SU(6) symmetric quark model predicts that this ratio should go to 1/2 when $x \to 1$, while if the interaction of the spectator quarks is defined by one gluon exchange, the ratio should go to zero.

The reach in x^* of the CLAS experiment was limited by the maximum beam energy of 5.7 GeV. With CLAS12 and 11 GeV electron beams, using the same low momentum proton tagging technique, the ratio of F_2^n/F_2^p will be measured up to $x^* \approx 0.8$.

V. NN SHORT RANGE CORRELATIONS

Understanding the short-range correlations (SRCs) in nuclei has been one of the persistent though rather elusive goals of nuclear physics for decades. The SRCs, produced by the NN interaction at distances less than the average inter-nucleon distance, result in a universal shape of the nuclear wave function for all nuclei at $p > p_F$, where p_F is the Fermi momentum (see, *e.g.* Ref. [13]). For quasi-elastic scattering, $A(e,e')$, x_B, Q^2, and the minimum recoil momentum of the $A-1$ system are related through energy and momentum conservation. For any nucleus A and fixed Q^2, there is a value of x_B^0 such that at $x_B > x_B^0$ the minimum recoil momentum contributing to the reaction exceeds the Fermi momentum, $p_m > p_F$. Therefore the cross section ratios for heavy and light nu-

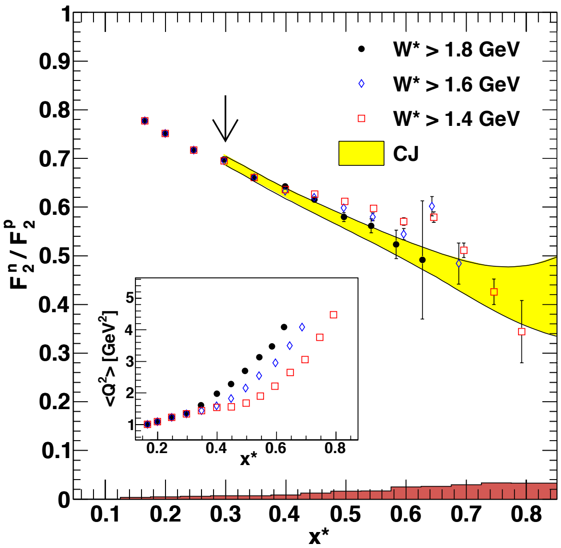

FIG. 6. Ratio F_2^n/F_2^p versus x^* for various lower limits on W^*. The data are compared with the recent parametrization from the CTEQ-Jefferson Lab (CJ global analysis [12]), with the upper and lower uncertainty limits indicated by the solid lines. The inset shows the average Q^2 as a function of x^* for each W^* cut. The arrow indicates the point at which the data are normalized to the CJ value. The resonance region ($W^* * < 2$ GeV) corresponds to $x^* \geq 0.4$, 0.5, and 0.6 for square, diamond, and circle points, respectively.

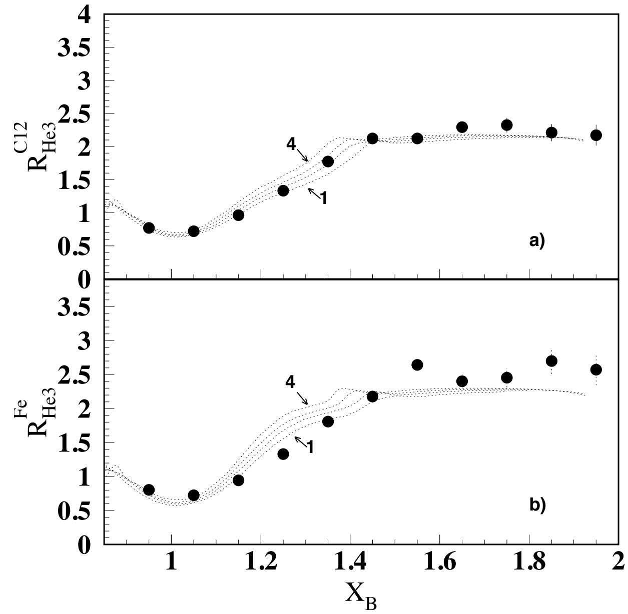

FIG. 7. R(A,^{3}He) as a function of x_B for $1.4 < Q^2 < 2.6$ GeV^2. Only statistical errors are shown. The curves are SRC model predictions for different Q^2 in the range 1.4 GeV^2 (curve 1) to 2.64 GeV^2 (curve 4), respectively, for (a) ^{12}C, (b) ^{56}Fe.

clei should be independent of x_B and Q^2 in the high recoil momentum region.

CLAS electroproduction data on ^{3}He, ^{4}He, ^{12}C, and ^{56}Fe targets were used to show the scaling behavior in the $2N$ and $3N$ SRC regions and to obtain the probability for NN SRCs in different nuclei [14, 15]. In Fig. 7 the x_B dependence of the weighted cross section ratios of ^{12}C and ^{56}Fe to ^{3}He for $Q^2 > 1.4$ GeV^2 are presented. The region of the scaling, $1.5 < x_B < 2$, corresponding to the region of NN SRC dominance in the nuclear wave function is clearly seen. The absolute probabilities of $2N$ SRCs were obtained by integration of the momentum distributions in deuterium and ^{3}He. It was found that the probability of short range correlations in nuclei relative to deuterium is ~ 3.8 times larger for ^{4}He and approximately 4.9 and 5.9 times larger for ^{12}C and ^{56}Fe, respectively.

VI. NEW PHYSICS OPPORTUNITIES WITH CLAS12

A new detector, CLAS12, soon will be commissioned in experimental Hall B with up to 11 GeV electron beams from the upgraded CEBAF machine at Jefferson Lab. CLAS12, as was its predecessor CLAS, is a large acceptance, multi-purpose detector capable of detecting and identifying neutral and charged particles in the full range of available momentum space. One of the key characteristics of the detector is its high luminosity, $L = 10^{35}$ cm^{-2}s^{-1}, an important parameter for executing a broad physics program. The approved physics program covers a wide range of studies of meson and baryon spectroscopy, nucleon and nuclear structure, quark propagation, and hadronization.

In addition to carrying over the established physics program of 6 GeV CLAS to a new kinematic domain, the energy of the upgraded CEBAF opens a new frontier inaccessible with the 6 GeV machine. The energy available for experiments is well above the J/ψ meson production threshold of 8.2 GeV. This opens a unique opportunity to explore the gluonic structure of the nucleon by studying charmonium photoproduction in the unmeasured near threshold region $E_\gamma < 11$ GeV. There is already an approved experiment with CLAS12 for studying near threshold J/ψ photoproduction. The same measurements access the energy range where the hidden charmed pentaquark states have been found by the LHCb Collaboration [16]. A variety of models predict sizable photoproduction cross sections for these pentaquarks, see e.g. Refs. [17, 18]. CLAS12 will be able not only to perform high precision measurements of J/ψ photoproduction near threshold, but also study photoproduction of these pentaquarks [19]. In Fig. 8 the expected results on J/ψ photoproduction cross sections as a function of photon energy are shown without and with the LHCb pentaquark states. In the simulation the lower limit for the $P_c^+(4450)$ cross section from Ref. [17] was used. The

CLAS12 measurements will shed light on the reaction mechanism near threshold, 2- vs. 3-gluon exchanges [20], and provide unique insights into the gluonic structure of the nucleon at large x.

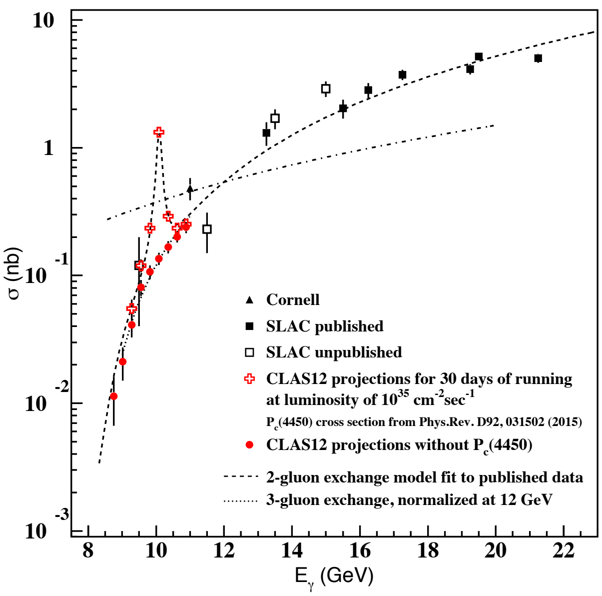

FIG. 8. Cross section of J/ψ photoproduction as a function of photon energy. The red points are the expected results from CLAS12 running for 30 days at its design luminosity with an 11 GeV electron beam.

VII. SUMMARY

The CLAS detector in experimental Hall B at Jefferson Lab produced a huge amount of cross section and polarization data using up to 6 GeV longitudinally polarized electron beams. A rigorous physics program for studying nucleon and nuclear structure, hadron spectroscopy, and in-medium effects has been executed over 15 years. One of the most significant achievements was the study of the spectrum of nucleon resonances and transition FFs, including studies with strangeness production. CLAS provided the lion's share of the world's data on meson photo- and electroproduction in the resonance excitation region. These data were not only important for identifying new states (accommodated in CQM and LQCD), but also in revealing structure of known resonances. Theoretical analyses of these results have revealed that there are two major contributions to the resonance structure: an internal quark core and an external meson-baryon cloud (see e.g. Ref. [21]). CLAS also provided a significant amount of data on spin (beam, target, double) asymmetries for meson production, pioneered measurements of Color Transparency using ρ-meson electroproduction [22], and studied Two-Photon Exchange (TPE) effects by comparing elastic $e^{+/-}p$ cross sections [23].

Most of this program will be continued with the upgraded CLAS12 detector and up to 11 GeV electron beams. With the available high energy beams, CLAS12 will complement the CLAS physics program with studies of charmonium production, Time-like Compton scattering, and meson spectroscopy.

This material is based upon work supported by the U.S. Department of Energy, Office of Science, Office of Nuclear Physics under contract DE-AC05-06OR23177.

[1] B.A. Mecking *et al.*, Nucl. Instr. Meth. A **440**, 263 (2000).
[2] S.J. Brodsky, D.S. Hwang, and I. Schmidt, Phys. Lett. B **530**, 99 (2002). J.C. Collins, Phys. Lett. B **536**, 43 (2002). X. Ji and F. Yuan, Phys. Lett. B **543**, 66 (2002).
[3] D. Müller, D. Robaschik, B. Geyer, F.-M. Dittes, and J. Horejsi, Fortschr. Phys. **42**, 101 (1994). X. Ji, Phys. Rev. Lett. **78**, 610 (1997); Phys. Rev. D **55**, 7114 (1997). A.V. Radyushkin, Phys. Lett. B **380**, 417 (1996); Phys. Rev. D **56**, 5524 (1997). J.C. Collins, L. Frankfurt, and M. Strikman, Phys. Rev. D **56**, 2982 (1997).
[4] S. Stepanyan *et al. (CLAS Collaboration)*, Phys. Rev. Lett. **87**, 182002 (2001).
[5] S. Chen *et al. (CLAS Collaboration)*, Phys. Rev. Lett. **97**, 072002 (2006).
[6] F.-X. Girod *et al. (CLAS Collaboration)*, Phys. Rev. Lett. **100**, 162002 (2008).
[7] S. Pisano *et al. (CLAS Collaboration)*, Phys. Rev. D **91**, 052014 (2015).
[8] H.S. Jo *et al. (CLAS Collaboration)*, Phys. Rev. Lett. **115**, 212003 (2015).
[9] M. Hattawy *et al. (CLAS Collaboration)*, to be published.
[10] J. Lachniet *et al. (CLAS Collaboration)*, Phys. Rev. Lett. **102**, 192001 (2009).
[11] N. Baillie *et al. (CLAS Collaboration)*, Phys. Rev. Lett. **108**, 142001 (2012).
[12] A. Accardi, W. Melnitchouk, J.F. Owens, M.E. Christy, and C.E. Keppel *et al.*, Phys. Rev. D **84**, 014008 (2011).
[13] L.L. Frankfurt and M.I. Strikman, Phys. Rep. **160**, 235 (1988).
[14] K.S. Egiyan *et al. (CLAS Collaboration)*, Phys. Rev. C **68**, 014313 (2003).
[15] K.S. Egiyan *et al. (CLAS Collaboration)*, Phys. Rev. Lett. **96**, 082501 (2006).

[16] R. Aaij *et al. (LHCb Collaboration)*, Phys. Rev. Lett. **115**, 072001 (2015).
[17] V. Kubarovsky and M.B. Voloshin, Phys.Rev. D **92**, 031502 (2015).
[18] Marek Karliner and Jonathan L. Rosner, arXiv:1508.01496.
[19] M. Battaglieri *et al.*, CLAS12 Note 2015-007 (2015).
[20] S.J. Brodsky, E. Chudakov, P. Hoyer, and J.M. Laget, Phys. Lett. B **498**, 23 (2001).
[21] Aznauryan, I. *et al.* J. Phys. Conf. Ser. **299**, 012008 (2011).
[22] L. El Fassi *et al. (CLAS Collaboration)*, Phys. Lett. B **712**, 326 (2012).
[23] D. Rimal *et al. (CLAS Collaboration)*, arXiv:1603.00315 (2016).